

# Isolated Boost DC-DC Converter with Reduced Switches for Fuel Cell Applications

Latha R<sup>1</sup>, Archana N<sup>2</sup>, Sri Vikram P<sup>3</sup>, Vishnu R<sup>4</sup>

{rla.eee@psgtech.ac.in<sup>1</sup>,naa.eee@psgtech.ac.in<sup>2</sup>,srivikram2001@gmail.com<sup>3</sup>,vishnurcks@gmail.com<sup>4</sup>}

Department of Electrical and Electronics Engineering, PSG college of Technology, Tamil Nadu, India

**Abstract.**For fuel cell applications, a unique isolated boost DC-DC converter with three switches is presented in this work. These are the primary attributes of the recommended converter: 1) Constant current input; 2) reduction in an active switch, addition of a diode, and a capacitor; 3) voltage waveforms on the transformer's primary and secondary sides remain intact when the duty cycle is altered; and 4) removal of the snubber circuit are some of the effects that should be observed. The operating principles, analysis, procedure for designing the converter's parameters, and simulation results are exhibited in this work.

**Keywords:**DC-DC power conversion, Voltage Double Rectifier (VDR), Step-up Transformer, Galvanic Isolation, Current-fed Full-Bridge (CFFB) converter

## 1 Introduction

Solar and wind energy are examples of renewable energy sources that are freely available, but because they are intermittent, their output is not reliable. But in case of Fuel cell, here the output is reliable and consistent through out the year since the fuel supply is consistent. Here, they produce heat as a by product, which raise the system's gross efficiency also can be used for co generation or heating [1]. Large-scale "step-up DC-DC conversion" methods are necessary for a number of applications, including uninterruptable power supply, solar PV systems, and fuel cells. Steep step-up voltage ratios and high conversion efficiencies are required for these applications [2]. Numerous studies and proposals for high step-up DC-DC converters have been made in an effort to transform knee-high voltages into a constant DC bus voltage. Voltage-fed full-bridge (VFFB) and current-fed full-bridge (CFFB) DC-DC converters are majorly involved in isolated topologies that offer galvanic isolation [14]. Due to the buck function of the voltage source converters, the primary potential gain of the VFFB DC-DC converters is provided as long as the large turn ratio and frequency transformer is used [4]. To enhance the capacity to boost voltage of the VFFB DC-DC converter, an active-clamped three-level rectifier or a boost converter is connected to the secondary side of the

device [5]. Due to the boost function included in the current-fed converters, the CFFB DC-DC converters are worthy for systems requiring a large step-up voltage gain [8].

Furthermore, CFFB converters have a lower input current ripple and turn ratio of the high-frequency transformer than VFFB DC-DC converters [15]. In order to reduce the voltage escalation that happens when the switch is turned off, which causes a greater loss of power, CFFB converters use a passive snubber [16]. Active clamping circuits which increase the size and the expense have been proposed to restore the CFFB converter's snubber's energy [9].

CFFB converters with soft-switching snubber-less naturally clamped have been proposed as a potential substitute for active clamping circuits. It was recommended to use an interleaved CFFB converter to reduce the input side current ripple [10]. By alternating two isolated CFFB converters, the number of components involving magnetic properties and the devices' current stress are reduced. For CFFB converter modules, the connection with an input series and output parallel was suggested to improve input sides' ability to block voltage and reduce the output sides' current ripple [11]. A distributed multi-transformer topology-based dual-input CFFB converter was introduced for the hybrid model of renewable energy systems [12]. These kinds of CFFB converters suggested, always employs more transformers and switches, which raises the system's loss that occurs and also the cost [13].

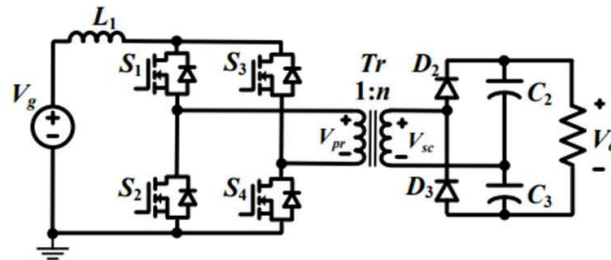


Fig 1. Traditional current-fed, four-switch, isolated boost DC-DC converter

Figure 1 illustrates a typical CFFB converter having a full bridge inverter, a voltage double rectifier, a step-up transformer with high frequency, connected to a resistive load, and also an inductor at the primary side for boosting properties. When just two of the switches—S1 and S4 or S2 and S3—are activated, the system operates in an energy-transfer mode. Additionally, when two switches (S1 and S4) or S2 and S3 are turned on, the input current decreases; however, the converter enters the boost mode and the input current rises when all switches are activated [20].

This study suggests a three-switch isolated boost DC-DC converter. The recommended converter uses only three switches which reduces the usage of one active switch, and causes the addition of one more diode, and one more capacitor in comparison to the typical CFFB converter. For the suggested converter, the guiding principles for parameter design, analysis, and operation are described. Also, the Results from the simulation that have been undertaken are given to validate the analysis.

## 2 Proposed Methodology

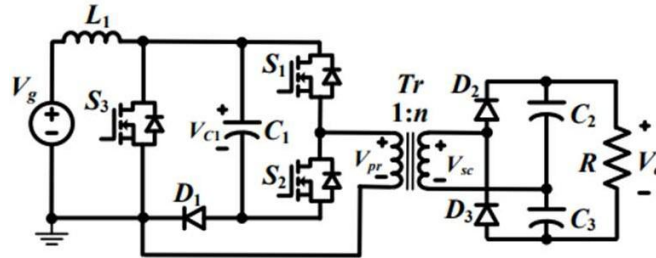


Fig 2. Proposed three-switch, isolated boost DC-DC converter

Figure 2 displays the circuit diagram for the suggested three-switch isolated boost DC-DC converter. The low-voltage side of the transformer consists of the transformer's primary winding ( $Tr$ ), three switches ( $S1$ ,  $S2$ , and  $S3$ ), an inductor for boosting properties ( $L1$ ), a capacitor ( $C1$ ), and a diode ( $D1$ ). The high-voltage side of the voltage double rectifier (VDR), which consists of two diodes ( $D2$  and  $D3$ ) and two capacitors ( $C2$  and  $C3$ ), is connected to the resistive load ( $R$ ) and the secondary winding of the transformer ( $Tr$ ). The main characteristics of the recommended converter are as follows: 1) Since there is little to no ripple in the DC current at the input side, there is no need to use an LC filter or a bank of decoupling capacitors in the fore front, which are usually employed to safeguard energy sources like fuel cells; 2) Here, it uses one more diode, one more capacitor, and one fewer active switch than a quintessential isolated DC-DC boost converter; 3) When the output voltage is adjusted, the high-frequency transformer's voltage wave form which is operating at high-frequency, at the primary side and secondary side remain unchanged, which makes high-frequency transformer design simpler; and 4) The snubber circuit is not necessary because the sudden increase in voltage can be controlled by fastening the voltage of the capacitor  $C1$ . The switch  $S2$ , that is suggested is no longer connected to the source ground, as seen in Fig.2. In this case, the proposed converter makes use of three gate drivers, each of which has unique, independent grounds. The conventional CFFB, isolated boost DC-DC converter shown in Figure 1 (which uses three distinct grounds for four gate drivers) is employed by both converters in the same number of ways.

### 2.1 Operating Principle

The suggested converter's circuit is analyzed under the following circumstances: 1) The CCM mode of operation of the inverter is used. 2) Each device is perfect and lossless. 3) An ideal transformer, along with a leakage inductor, are used to mimic the high-frequency transformer. 4) Linear changes in the amount of current flowing through the transformer's and inductor's windings. 5) The capacitors' capacitance is adequate to sustain a prolonged steady capacitor voltage. 6) The parasitic capacitances and leakage inductance oscillations are not taken into account. 7) Switch  $S3$ 's duty cycle is  $D$ , while  $DA$  is its minimum value. By setting  $DA$  to 0.3, for an AC pulse, the voltage waveforms at the transformer's high-

frequency primary and secondary sides are kept at 30% positive, 20% zero, 30% negative, and 20% zero, respectively. The range of [0.25, 0.5] is where DA should be for optimal transformer utilization. The converter's least voltage gain determines which DA to use. By placing a capacitor C1 between the input side inductor and the leakage inductor of the transformer, the snubber circuit is removed in the suggested converter. When the inductor at the input side transitions from the stored to the transferred energy state, the current flowing through it does not change suddenly because of the capacitor C1 that connects between it and the leakage inductor. Therefore, the recommended converter does not require a snubber circuit. Here, Hard switching disables the S3 switch, causing S3 to experience an overstress voltage. As was mentioned in, the isolated boost converter's major switches typically have voltage ratings of twice or thrice the input side's maximum voltage. Consequently, the S3 switch experiences stress that is less than three times the topmost voltage at the input side. The stray inductances in the circuit are what cause this overstress.

## **2.2 Pulse Width Modulation Control**

In order to increase the time that S1 is continually "ON," an additional state in which S1 and S3 are switched "ON" concurrently is placed into the zero state. The signals used to control the switch, S3, are produced by comparing a high-frequency triangular waveform,  $V_{tri}$ , to the reference voltage,  $V_{ref}$ . To create signals that will be used for controlling the switches S1 and S2, here  $V_{tri}$  is compared to a second reference voltage with an amplitude of  $(1 - V_{ref})$ . Then the control voltage,  $V_{con}$ , is contrasted with  $V_{tri}$  in order to produce the additional states. Note that  $V_{con}$  is in the range  $[1 - V_{ref}, V_{ref}]$  to ensure that the additional state is only inserted into the zero state. Here, in this suggested converter,  $V_{ref}$  is typically maintained constant for the transformer's constant voltage waveforms. As a result,  $V_{con}$  serves as the converter's sole control voltage.

## **3 Simulations and Experimental Results**

### **3.1 Simulation Results**

Following parameters were used in a PSIM simulation to test the suggested converter's working principle:  $L1 = 1\text{mH}$ ,  $C1 = 220\mu\text{F}$ ,  $C2 = C3 = 150\mu\text{F}$ , and  $R = 600\Omega$ . MOSFETs were configured with an  $8\text{m}\Omega$  drain-to-source on-resistance. The diodes' forward voltage was set at 0.7V. The transformer, which operates at high frequency, had a turn ratio of 2.5. The magnetic inductance, as computed from the primary side of the transformer, was determined to be 1.4 mH. A leakage inductance value of  $11\mu\text{H}$  was chosen. The output voltage was 400V, and the frequency of switching was set at 10kHz. There is a  $2\mu\text{s}$  dead band gap between switches S1 and S2. The simulation parameters chosen for the suggested boost converter topology are clearly shown in Table 1.

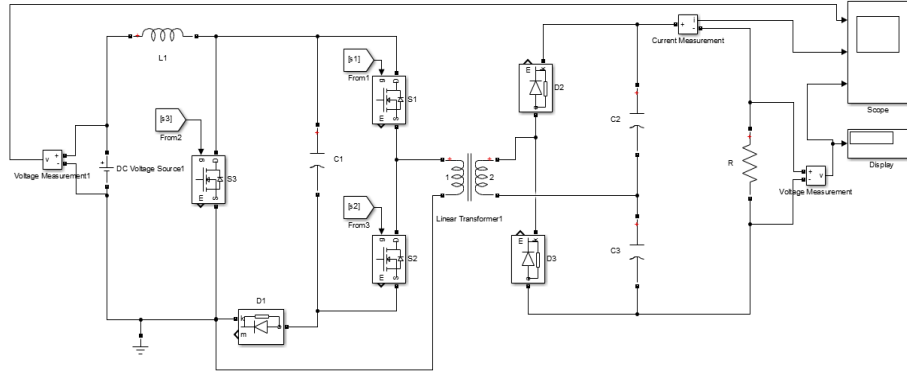


**Fig 3.** Simulation of the Proposed Converter

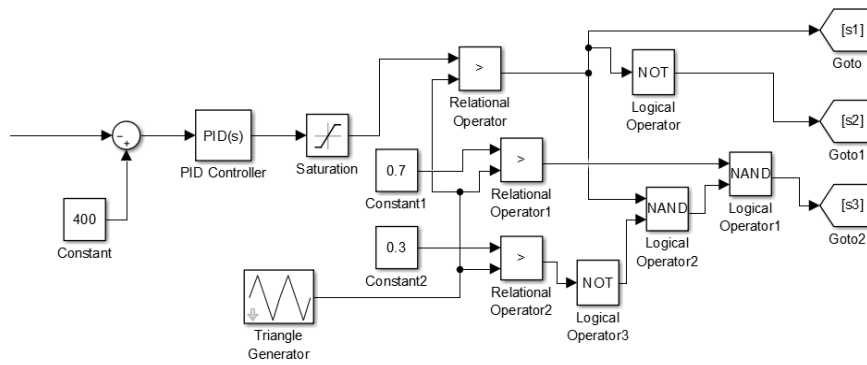


**Fig 4.** Simulation of Closed loop Control using PID Controller

**Table 1.** Proposed Converter's Expertial And Simulative Parameters

Range of input voltage ( $V_g$ )		40-60V
Resultant voltage( $V_0$ )		400V
Inductor( $L_1$ )		1mH
Transformer	Turn ratio	1:2:5
	Inductance at Primary side	1.4mH
	Leakage inductance	11 $\mu$ H
Capacitors	$C_1$	220 $\mu$ F
	$C_2=C_3$	150 $\mu$ F
Frequency of switching		10kHz
Resistive load(R)		600 $\Omega$

The outcomes of the simulation run for the suggested converter are shown in Figure 5 at  $V_g = 60$  V. 1.71 A is the peak-to-peak ripple of the constant input current. The transformer's principal voltage is divided into three levels. The outcomes of the simulation run for the suggested converter are shown in Figure 5. The transformer's primary and secondary voltage waveforms remain unchanged in the event that the input side voltage fluctuates between its maximum and minimum values. These simulations' outcomes concur with the theoretical analysis.

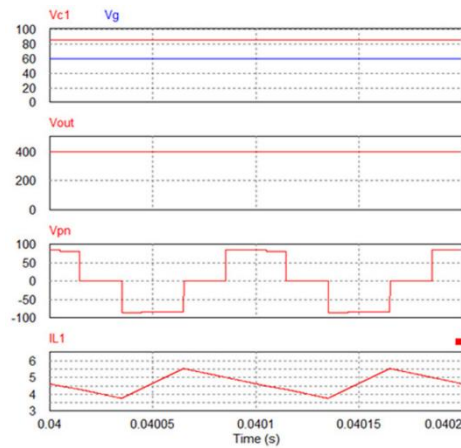


**Fig 5(a).** Simulation Results

Outcomes of the simulation at  $V_g = 60$  V. In this instance, 5(a) from top to bottom: capacitor and input voltages, output voltage, primary voltage of the transformer, and input current;

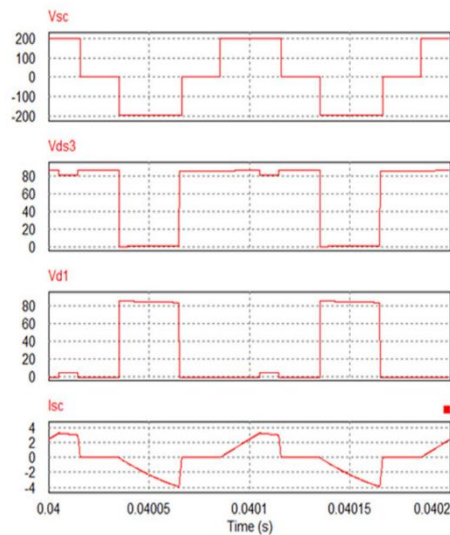


**Fig 5(b).** Simulation Results

In this instance, 5(b) Secondary voltage of the transformer, drain–source voltage of S3, diode D1 voltage, and secondary current of the transformer;

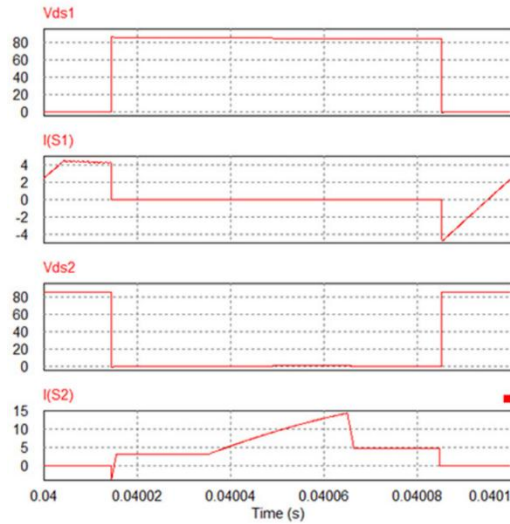


**Fig 5(c).** Simulation Results

In this instance, 5(c) drain–source voltage of S1, drain–source current of S1, drain–source voltage of S2, and drain–source current of S2.

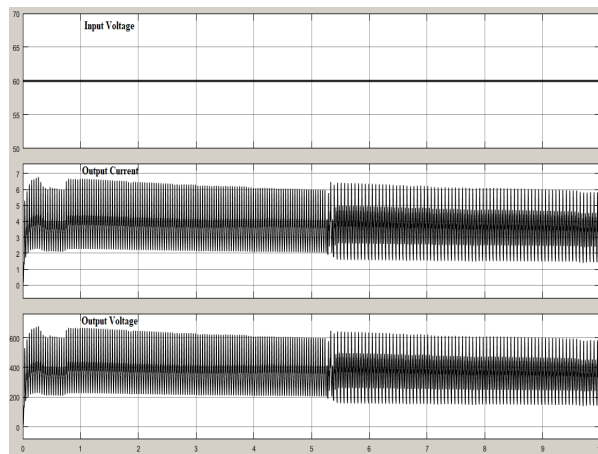


**Fig 6.** Outcomes of simulation: Input Voltage, Output Current and Output Voltage

## 4 Conclusion

This work proposed a novel isolated three-switch boost DC-DC converter. The transformers' voltage waveform at the primary side and secondary side are unaltered, there is no snubber circuit, there is a reduced number of active switches used and has

continuous input current in the suggested converter. This converter has the following drawbacks as compared to the traditional CFFB converter: it requires an additional diode and capacitor, has a heavy input current ripple, and operates in hard switching. The operational tenets, analysis, and outcomes of the closed loop simulation are provided. With a constant input current and galvanic isolation, the proposed converter can be applied to a variety of applications, such as fuel cells, where a fluctuating low-dc input voltage needs to be increased to a high fixed voltage at the output side.

## References

- [1] D. S. Gautam, F. Musavi, W. Eberle, and W. G. Dunford, "A zero-voltage switching full-bridge dc–dc converter with capacitive output filter for plug-in hybrid electric vehicle battery charging," *IEEE Trans. Power Electron.*, vol. 28, no. 12, pp. 5728–5735, Dec. 2013.
- [2] Y. Xie, R. Ghaemi, J. Sun, and J. S. Freudenberg, "Implicit model predictive control of a full bridge dc–dc converter," *IEEE Trans. Power Electron.*, vol. 24, no. 12, pp. 2704–2713, Dec. 2009.
- [3] P. Sun, L. Zhou, and K. M. Smedley, "A reconfigurable structure dc–dc converter with wide output range and constant peak power," *IEEE Trans. Power Electron.*, vol. 26, no. 10, pp. 2925–2935, Oct. 2011.
- [4] B. Gu, J. S. Lai, N. Kees, and C. Zheng, "Hybrid-switching full-bridge dc–dc converter with minimal voltage stress of bridge rectifier, reduced circulating losses, and filter requirement for electric vehicle battery chargers," *IEEE Trans. Power Electron.*, vol. 28, no. 3, pp. 1132–1144, March 2013.
- [5] C. Yao, X. Ruan, and X. Wang, "Isolated buck-boost dc/dc converters suitable for wide input-voltage range," *IEEE Trans. Power Electron.*, vol. 26, no. 9, pp. 2599–2613, Sep. 2011.
- [6] C. Yao, X. Ruan, and X. Wang, "Automatic mode-shifting control strategy with input voltage feed-forward for full-bridge-boost dc–dc converter suitable for wide input voltage range," *IEEE Trans. Power Electron.*, vol. 30, no. 3, pp. 1668–1682, March 2015.
- [7] H. Wu, Y. Lu, K. Sun, and Y. Xing, "Phase-shift controlled isolated buck-boost converter with active-clamped three-level rectifier (AC-TLR) featuring soft-switching within wide operation range," *IEEE Trans. Power Electron.*, vol. 31, no. 3, pp. 2372–2386, Mar. 2016.
- [8] R. Y. Chen, T. J. Liang, J. F. Chen, R. L. Lin, and K. C. Tseng, "Study and implementation of a current-fed full-bridge boost dc–dc converter with zero-current switching for high-voltage applications," *IEEE Trans. Ind. Appl.*, vol. 44, no. 4, pp. 1218–1226, July/Aug. 2008.
- [9] S. Jalbrzykowski and T. Citko, "Current-fed resonant full-bridge boost dc/ac/dc converter," *IEEE Trans. Ind. Electron.*, vol. 55, no. 3, pp. 1198–1205, March 2008.
- [10] X. Kong, and A. M. Khambadkone, "Analysis and implementation of a high efficiency, interleaved current-fed full bridge converter for fuel cell system," *IEEE Trans. Power Electron.*, vol. 22, no. 2, pp. 543–550, March 2007.
- [11] A. Mohammadpour, L. Parsa, M. H. Todorovic, R. Lai, R. Datta, and L. Garces, "Series-input parallel-output modular-phase dc–dc converter with soft-switching and high-frequency isolation," *IEEE Trans. Power Electron.*, vol. 31, no. 1, pp. 111–119, Jan. 2016.
- [12] Z. Zhang, O. C. Thomsen, M. A. E. Andersen, and H. R. Nielsen, "Dual-input isolated full-bridge boost dc-dc converter based on the distributed transformers," *IET Power Electron.*, vol. 5, no. 7, pp. 1074–1083, Aug. 2012.



- [13] Z. Zhang, O. C. Thomsen, and M. A. E. Andersen, "Soft-switched dual-input dc-dc converter combining a boost-half-bridge cell and a voltage-fed full-bridge cell," *IEEE Trans. Power Electron.*, vol. 28, no. 11, pp. 4897-4920, Nov. 2013.
- [14] M. Nymand, and M. A. E. Andersen, "High-efficiency isolated boost dc-dc converter for high-power low-voltage fuel-cell applications," *IEEE Trans. Ind. Electron.*, vol. 57, no. 2, pp. 505-514, Feb. 2010.
- [15] Z. Lizhi "A novel soft-commutating isolated boost full-bridge ZVSPWM dc-dc converter for bidirectional high power applications," *IEEE Trans. Power Electron.*, vol. 21, no. 2, pp. 422-429, Feb. 2006.
- [16] A. Mousavi, P. Das, and G. Moschopoulos, "A comparative study of a new ZCS dc-dc full-bridge boost converter with a ZVS active-clamp converter," *IEEE Trans. Power Electron.*, vol. 27, no. 3, pp. 1347-1358, March 2012.
- [17] U. R. Prasanna, and A. K. Rathore, "Extended Range ZVS Active-Clamped Current-Fed Full-Bridge Isolated DC/DC Converter for Fuel Cell Applications: Analysis, Design, and Experimental Results," *IEEE Trans. Ind. Electron.*, vol. 60, no. 7, pp. 2661-2672, July 2013.
- [18] M. Baei, M. Narimani, and G. Moschopoulos, "A new ZVS-PWM full-bridge boost converter," *Journal of Power Electronics*, vol. 14, no. 2, pp. 237-248, March 2014.
- [19] M. Mohr, and F. W. Fuchs, "Clamping for current-fed dc/dc converters with recovery of clamping energy in fuel cell inverter systems," in *Proc. European Conf. Power Electron. and Applicat. (EPE)*, 2-5 Sept. 2007, pp. 1-10.
- [20] P. Xuwei, A. K. Rathore, and U. R. Prasanna, "Novel soft-switching snubberless naturally clamped current-fed full-bridge front-end-converter-based bidirectional inverter for renewables, microgrid, and UPS applications," *IEEE Trans. Ind. Appl.*, vol. 50, no. 6, pp. 4132-4141, Nov/Dec. 2014.